Longitudinal diffusion MRI for treatment response assessment: Preliminary experience using an MRI-guided tri-cobalt 60 radiotherapy system

Yingli Yang,[a] Minsong Cao, Ke Sheng, Yu Gao, Allen Chen, Mitch Kamrava, Percy Lee, Nzhde Agazaryan, James Lamb, David Thomas, and Daniel Low
Department of Radiation Oncology, University of California, Los Angeles, California 90095

Peng Hu
Department of Radiological Sciences, University of California, Los Angeles, California 90095

(Received 7 December 2015; revised 3 February 2016; accepted for publication 6 February 2016; published 23 February 2016)

Purpose: To demonstrate the preliminary feasibility of a longitudinal diffusion magnetic resonance imaging (MRI) strategy for assessing patient response to radiotherapy at 0.35 T using an MRI-guided radiotherapy system (ViewRay).
Methods: Six patients (three head and neck cancer, three sarcoma) who underwent fractionated radiotherapy were enrolled in this study. A 2D multislice spin echo single-shot echo planar imaging diffusion pulse sequence was implemented on the ViewRay system and tested in phantom studies. The same pulse sequence was used to acquire longitudinal diffusion data (every 2–5 fractions) on the six patients throughout the entire course of radiotherapy. The reproducibility of the apparent diffusion coefficient (ADC) measurements was assessed using reference regions and the temporal variations of the tumor ADC values were evaluated.
Results: In diffusion phantom studies, the ADC values measured on the ViewRay system matched well with reference ADC values with <5% error for a range of ground truth diffusion coefficients of $0.4–1.1\times10^{-3}$ mm^2/s. The remote reference regions (i.e., brainstem in head and neck patients) had consistent ADC values throughout the therapy for all three head and neck patients, indicating acceptable reproducibility of the diffusion imaging sequence. The tumor ADC values changed throughout therapy, with the change differing between patients, ranging from a 40% drop in ADC within the first week of therapy to gradually increasing throughout therapy. For larger tumors, intratumoral heterogeneity was observed. For one sarcoma patient, postradiotherapy biopsy showed less than 10% necrosis score, which correlated with the observed 40% decrease in ADC from the fifth fraction to the eighth treatment fraction.
Conclusions: This pilot study demonstrated that longitudinal diffusion MRI is feasible using the 0.35 T ViewRay MRI. Larger patient cohort studies are warranted to correlate the longitudinal diffusion measurements to patient outcomes. Such an approach may enable response-guided adaptive radiotherapy. © *2016 American Association of Physicists in Medicine.* [http://dx.doi.org/10.1118/1.4942381]

Key words: MRI-guided radiotherapy, diffusion MRI, ADC, treatment response, adaptive therapy

1. INTRODUCTION

Diffusion magnetic resonance imaging (MRI) is a promising imaging technique for prediction of tumor response to radiation therapy,[1,2] earlier than traditional tumor size/morphology-based response signatures.[3] Baseline apparent diffusion coefficient (ADC) or changes in ADC values between baseline and post-therapy time points have been shown to correlate with tumor control and patient outcome after radiotherapy.[4–7] Therefore, diffusion MRI-based early response assessment holds great promises for adaptive radiotherapy, wherein the treatment plan would be altered during therapy based on individual patient's response. Such an adaptive therapy strategy may support dose escalation for radioresistant tumors or tumor subregions to improve locoregional tumor control, or to de-escalate dose for well responding tumor subregions, reducing surrounding critical structure toxicity.[8]

Despite its potential, diffusion MRI-based adaptive radiotherapy has not been adopted. This is because, at least in part, the optimal image timing has not been developed. In some diffusion MRI studies for radiation therapy, diffusion imaging was performed once before therapy, and another time at weeks to months after therapy.[5,9] In several studies, diffusion MRI was also performed early during the course of radiotherapy.[6,7,10] The results of these studies point to promising role of diffusion MRI for predicting tumor response. However, these approaches may not adequately characterize the temporal changes in diffusion. For example, a single diffusion imaging during therapy could be too late for early responders or too early for late responders. Furthermore, a single diffusion measurement is sensitive to measurement errors and noise at a single time point.

Because the optimal timing of diffusion MRI acquisition has not been determined, we have elected to acquire the

diffusion image data at relatively high frequency, e.g., every 3–5 fractions. Recently, a real-time MRI-guided radiotherapy system combining a 0.35 T MRI system and three cobalt 60 heads (MRIdian System™, ViewRay™, Cleveland, OH, USA) has become commercially available. The novel system combines real-time MRI-based tumor motion tracking with radiation therapy capability in a single gantry.[11] We hypothesize that such a hybrid MRI-radiotherapy system may eliminate many of the practical and scientific challenges and bring diffusion MRI-guided adaptive radiation therapy closer to widespread clinical utility. In this work, we report our early experience of diffusion MRI at the ViewRay 0.35 T low field MRI system and demonstrate its feasibility in longitudinal tumor response assessment in a small cohort of patients undergoing radiotherapy.

2. METHODS

We implemented a spin echo (SE)-based diffusion sequence on the ViewRay 0.35 T MRI system using a single-shot echo planar imaging (EPI) k-space sampling scheme, a commonly used strategy at higher field strengths,[12,13] with a maximum gradient amplitude of 18 mT/m and a maximum gradient slew rate of 200 mT/(m/ms). As a comparison, the state-of-the-art higher field systems typically have a maximum gradient amplitude of 40–80 mT/m and a maximum gradient slew rate of at least 200 mT/(m/ms). A whole-body radiofrequency (RF) coil was used for transmission and a flexible surface coil was used to receive the MRI signal. The same sequence was used for both phantom and *in vivo* studies.

2.A. Phantom study

The SE-EPI sequence was used to acquire single-slice diffusion images with b-values of 0–500 with 100 mm^2/s increments using a commercially available diffusion phantom (Model 128, High Precision Devices, Inc., Boulder, CO), which contained 13 vials filled with aqueous solutions of polyvinylpyrrolidone of increasing concentrations. The ADC values of the vials were calculated using a standard exponential fit of the mean signal intensity for each vial relative to the b values. The calculated ADC values were compared with the reference ADC values provided by the phantom manufacturer using a commercial 3 T system.

2.B. *In vivo* study

Under an Institutional Review Board approved protocol, a total of six patients were recruited in this study, including three head and neck cancer and three sarcoma patients. Individual written informed consents were obtained prior to the MRI study. While all of the patients underwent the imaging protocol, they were not all treated using the ViewRay system; the three head and neck patient and one sarcoma patient were treated using the ViewRay system and two sarcoma patients were treated using Truebeam™ (Varian Medical Systems, Inc, Corona, CA, USA) and Tomotherapy™ (Accuray™, Sunnyvale, CA, USA), respectively. All patients underwent conventionally fractionated IMRT. For patients who were treated on the ViewRay system, imaging was performed immediately after the treatment while the patient was in the treatment position on the ViewRay patient couch. For patients undergoing therapy on the other systems, the patient was brought to the ViewRay system and imaged immediately following his/her treatment. The treatment position was reproduced on the ViewRay, aligning to the positioning lasers. The diffusion images were acquired every 2–5 fractions throughout the treatment during free breathing. For each imaging session, ten slices were acquired interleaved with the different b-values covering the gross tumor volume (GTV), which was typically positioned near the isocenter. The pulse sequence parameters included: flip angle = 90°, echo time (TE) = 160 ms, repetition time (TR) = 2600 ms, slice thickness = 6 mm, EPI factor = 128, field of view (FOV) = 350×350 mm, b-values = 0, 100, 200, 300, 400, 500 mm^2/s, 5 averages and total scan time of 70 s for all ten slices. The diffusion images were processed to obtain the ADC maps for each slice using standard exponential fitting for each voxel. The $b = 100$ images were excluded from our exponential fitting to reduce microvascular perfusion effects.[14] Regions of interest (ROIs) were drawn in the tumor on the diffusion images based on each patient's clinical GTV contours. A separate reference ROI was drawn in the brain stem for the three head and neck cancer patients. The ADC values for these reference ROIs were not expected to change over the course of the treatment and were used to assess the reproducibility of our ADC measurements.

3. RESULTS

3.A. Phantom study

The differences between our ADC measurements at 0.35 T and the reference ADC values measured on 3 T were less than 5% across the ADC range of $0.4–1.1\times10^{-3}$ mm^2/s. These phantom results confirmed that SE-EPI diffusion sequence on ViewRay provided accurate ADC measurements.

3.B. *In vivo* study

Each patient successfully underwent 4–7 diffusion MRI scans depending on their treatment length. Figure 1 shows ADC maps from a 45 yr old patient (Patient #1) with squamous cell carcinoma at the left maxillary sinus acquired at seven time points during the course of treatment. The brainstem ADC values remained stable throughout the treatment with a mean brainstem ADC between 0.47×10^{-3} and 0.57×10^{-3} mm^2/s for all seven time points, which confirmed the ADC measurement reproducibility. The mean ADC for the tumor increased from 1.3×10^{-3} mm^2/s at the fourth fraction to 1.6×10^{-3} mm^2/s at the 31st fraction. In another head and neck cancer patient (Patient #2) shown in Fig. 2, the brainstem ADC values also remained relatively stable throughout the treatment (between 0.49×10^{-3} and 0.56×10^{-3} mm^2/s); however, the tumor ADC value substantially decreased from 1.5×10^{-3} mm^2/s at the second fraction of the treatment to 1.0×10^{-3} mm^2/s at the 29th fraction (33% reduction).

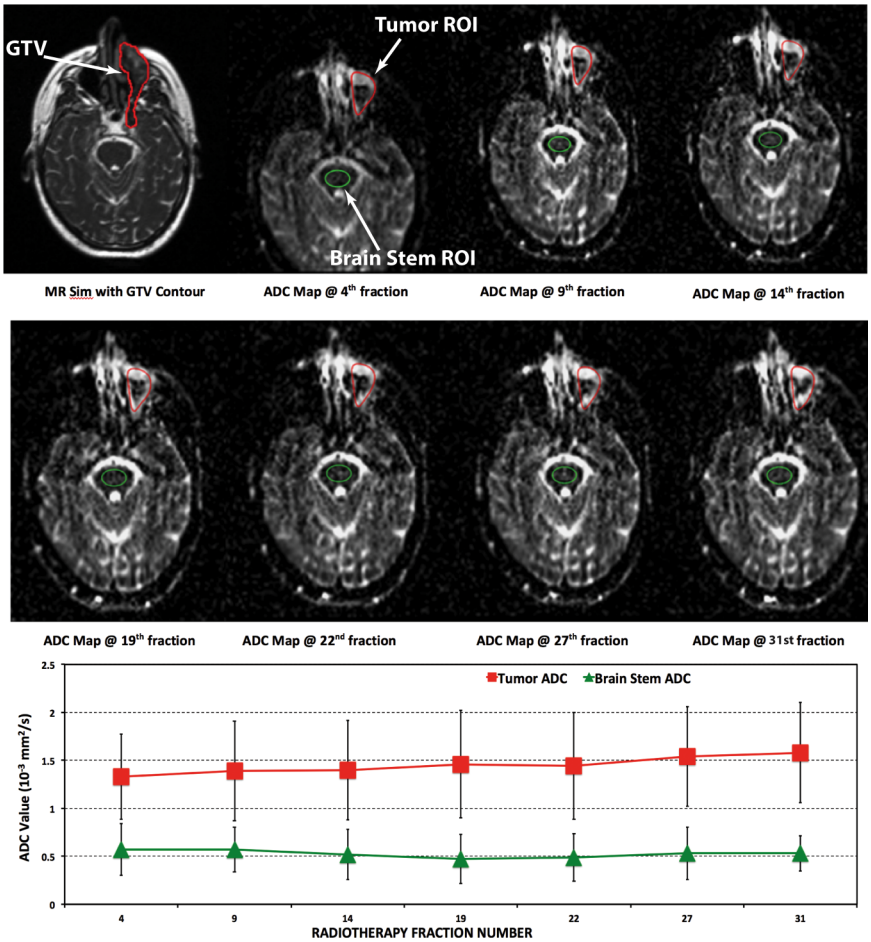

FIG. 1. Longitudinal diffusion data from a 45 yr old head and neck cancer patient (Patient #1). The error bars indicate standard deviations within the ROI. The brain stem ADC values did not significantly change over the course of the treatment with a nonsignificant linear fit slope of -0.002×10^{-3} mm^2/s per day, which is expected. For this patient, the average tumor ADC increased consistently over time from 1.3×10^{-3} to 1.6×10^{-3} mm^2/s.

We hypothesize that for large tumors, our ADC maps may be used to assess localized treatment response for tumor subregions. Figure 3 shows a sarcoma patient (Patient #4) with a $32\times22\times14$ cm^3 tumor. The simulation CT image [Fig. 3(a)] did not differentiate well between tumor and surrounding normal tissue. The diffusion-weighted image [Fig. 3(b), $b=500$] clearly shows the hyperintense tumor that matched well with the patient's GTV contour, which was drawn by a clinical radiation oncologist based on the simulation CT. In the corresponding ADC map [Fig. 3(c)], there was considerable heterogeneity within the tumor with a mean ADC of 1.34×10^{-3} mm^2/s and a standard deviation of 0.41×10^{-3} mm^2/s within the GTV contour. The ADC values within the right lateral region of the tumor had much higher ADC values than other regions.

In another patient (Patient #5) with pleomorphic liposarcoma in the right forearm who underwent eight fractions of radiotherapy on the ViewRay system, we acquired four diffusion images at the time of MR simulation and at the second, fifth, and eighth fractions. The ADC values dropped from 1.56×10^{-3} to 1.12×10^{-3} mm^2/s during the course of treatment (1.56×10^{-3}, 1.48×10^{-3}, 1.45×10^{-3}, and 1.12×10^{-3} mm^2/s at MR simulation and at the second, fifth, and eighth fractions, respectively). The patient underwent biopsy 47 days after radiation therapy, which showed a necrosis score of less than 10%, an indication of poor response to the treatment. The patient's diagnostic MRI one month after radiation therapy also indicated tumor progression with an increase in size from $5.1\times3.1\times14.8$ to $6.2\times4.8\times13.9$ cm^3.

4. DISCUSSION

In this work, we demonstrate for the first time the preliminary feasibility of a longitudinal diffusion MRI strategy at 0.35 T for patients undergoing fractionated radiotherapy using an integrated MRI-radiotherapy system. In addition to demonstrating the feasibility of low field diffusion imaging, to our knowledge, this was the first study reporting diffusion MRI data acquired every 2–5 fractions throughout the entire course of radiotherapy. Although previous studies demonstrated ADC changes at 1–3 weeks into the therapy and 3–8 weeks after therapy for responding tumors,[5–7,9,10] the imaging frequency did not allow a systematic study to determine the nonlinear temporal response and optimal timing for the treatment response prediction due to coarse temporal sampling. Furthermore, the temporal response of individual patients may be highly variable and sampling the diffusion at finer time

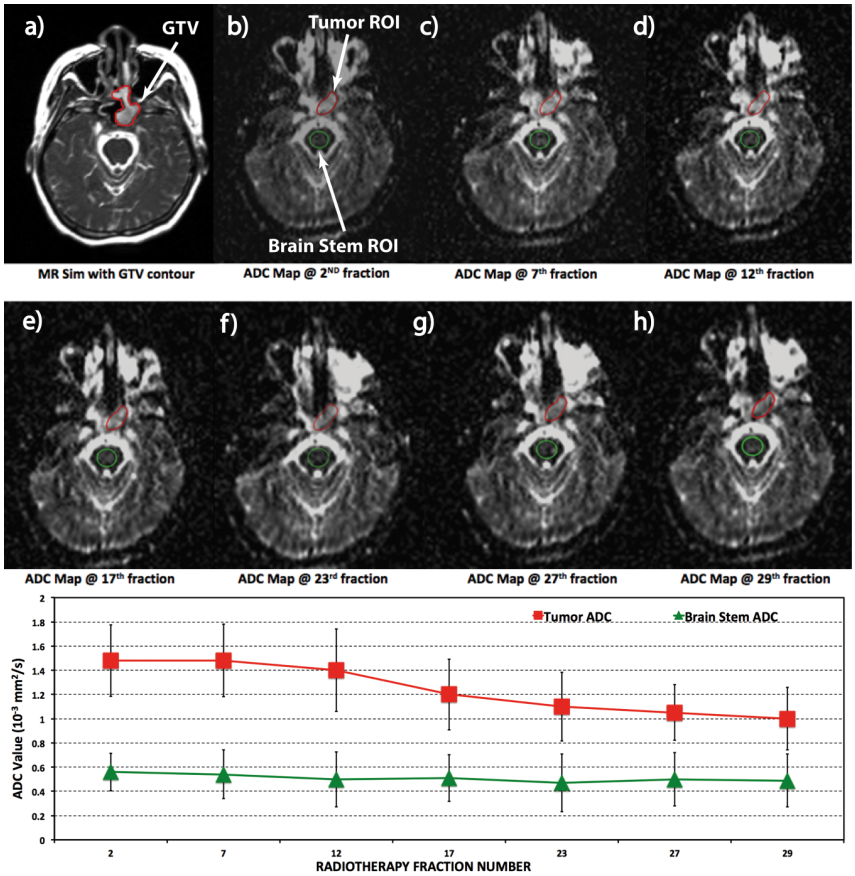

FIG. 2. Longitudinal diffusion data of a 51 yr old head and neck cancer patient (Patient #2). The error bars indicate standard deviations within the ROI. The average tumor ADC was relatively constant ($\sim 1.5\times10^{-3}$ mm^2/s) during the first three weeks of radiotherapy, and decreased to 1×10^{-3} mm^2/s from week 4 until the end of treatment. The ADC of the brainstem was relatively constant throughout the treatment with a nonsignificant linear fit slope of -0.001×10^{-3} mm^2/s per day.

intervals may facilitate individualized adaptive therapy. Based on our preliminary experiences in six patients, the proposed longitudinal diffusion MRI demonstrated different patterns of temporal variations and intratumoral spatial heterogeneities in ADC values. A larger patient cohort and follow-up study is clearly warranted to correlate our longitudinal diffusion imaging findings with patient outcome data. Nevertheless, our longitudinal diffusion MRI strategy, once validated in a larger cohort of patients, may represent a new paradigm of diffusion MRI guidance for adaptive radiotherapy, wherein the diffusion imaging is performed while the patient is on the treatment couch in the same position as therapy.

The magnetic field strength of the ViewRay system is 0.35 T to minimize the electron return effect and maximize spatial imaging accuracy.[15] Low field strength typically results in lower signal-to-noise ratio (SNR) efficiency; however, the $T1$ relaxation rates of tissues typically decrease with field strength, partially canceling SNR loss, and the diffusion EPI readouts may potentially benefit from low field due to the reduced absolute off-resonance frequencies. Our low-field ADC measurements agreed well with values in the literature that were acquired at higher field strengths.[10] The conventional MRI exams are typically performed on a stand-alone diagnostic MRI system with 1.5 T or higher field

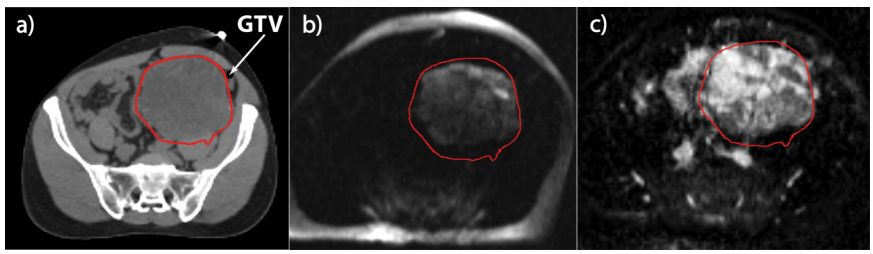

FIG. 3. (a) Simulation CT for a sarcoma patient (Patient #4) who underwent radiotherapy using the ViewRay system. The simulation CT shows good delineation of bony structures, but did not differentiate tumor from the surrounding normal tissue. (b) Diffusion weighted image of the patient with $b = 500$ mm^2/s where the tumor is hyperintense and is clearly differentiated from the surrounding tissue. (c) The ADC map of the same patient demonstrating great heterogeneity of ADC values within the tumor.

strength.[2,16,17] Due to the fact that imaging and therapy are on separate systems that are often operated by different clinical departments, it is impractical to perform longitudinal diffusion imaging during radiation therapy due to challenges in scheduling and logistics. In addition, the images need to be coregistered to the treatment simulation MRI or CT images, a step that introduces additional errors. MRI-guided radiotherapy systems, including the ViewRay system and other systems that are currently under development,[18] eliminate the aforementioned challenges and may enable longitudinal diffusion MRI in clinical workflow of radiotherapy.

[a]Author to whom correspondence should be addressed. Electronic mail: yyang@mednet.ucla.edu

[1]P. Bhatnagar, M. Subesinghe, C. Patel, R. Prestwich, and A. F. Scarsbrook, "Functional imaging for radiation treatment planning, response assessment, and adaptive therapy in head and neck cancer," RadioGraphics **33**, 1909–1929 (2013).

[2]C. Tsien, Y. Cao, and T. Chenevert, "Clinical applications for diffusion magnetic resonance imaging in radiotherapy," Semin. Radiat. Oncol. **24**, 218–226 (2014).

[3]A. A. Malayeri, R. H. El Khouli, A. Zaheer, M. A. Jacobs, C. P. Corona-Villalobos, I. R. Kamel, and K. J. Macura, "Principles and applications of diffusion-weighted imaging in cancer detection, staging, and treatment follow-up," RadioGraphics **31**, 1773–1791 (2011).

[4]G. Decker *et al.*, "Intensity-modulated radiotherapy of the prostate: Dynamic ADC monitoring by DWI at 3.0 T," Radiother. Oncol. **113**, 115–120 (2014).

[5]J. Il Yu, H. C. Park, D. H. Lim, Y. Choi, S. H. Jung, S. W. Paik, S. H. Kim, W. K. Jeong, and Y. K. Kim, "The role of diffusion-weighted magnetic resonance imaging in the treatment response evaluation of hepatocellular carcinoma patients treated with radiation therapy," Int. J. Radiat. Oncol., Biol., Phys. **89**, 814–821 (2014).

[6]F. Kuang, Z. Yan, J. Wang, and Z. Rao, "The value of diffusion-weighted MRI to evaluate the response to radiochemotherapy for cervical cancer," Magn. Reson. Imaging **32**, 342–349 (2014).

[7]S. Kim, L. Loevner, H. Quon, E. Sherman, G. Weinstein, A. Kilger, and H. Poptani, "Diffusion-weighted magnetic resonance imaging for predicting and detecting early response to chemoradiation therapy of squamous cell carcinomas of the head and neck," Clin. Cancer Res. **15**, 986–994 (2009).

[8]P. Kupelian and J.-J. Sonke, "Magnetic resonance-guided adaptive radiotherapy: A solution to the future," Semin. Radiat. Oncol. **24**, 227–232 (2014).

[9]L. Liu, N. Wu, H. Ouyang, J.-R. Dai, and W.-H. Wang, "Diffusion-weighted MRI in early assessment of tumour response to radiotherapy in high-risk prostate cancer," Br. J. Radiol. **87**, 20140359 (2014).

[10]A. D. King, K.-K. Chow, K.-H. Yu, F. K. F. Mo, D. K. W. Yeung, J. Yuan, K. S. Bhatia, A. C. Vlantis, and A. T. Ahuja, "Head and neck squamous cell carcinoma: Diagnostic performance of diffusion-weighted MR imaging for the prediction of treatment response," Radiology **266**, 531–538 (2013).

[11]S. Mutic and J. F. Dempsey, "The ViewRay system: Magnetic resonance-guided and controlled radiotherapy," Semin. Radiat. Oncol. **24**, 196–199 (2014).

[12]F. Barchetti, N. Pranno, G. Giraldi, A. Sartori, S. Gigli, G. Barchetti, L. Lo Mele, and L. T. Marsella, "The role of 3 Tesla diffusion-weighted imaging in the differential diagnosis of benign versus malignant cervical lymph nodes in patients with head and neck squamous cell carcinoma," BioMed Res. Int. **2014**, Article ID 532095 (9pp.) (2014).

[13]L. Mannelli, S. Nougaret, H. A. Vargas, and R. K. G. Do, "Advances in diffusion-weighted imaging," Radiol. Clin. North Am. **53**, 569–581 (2015).

[14]D. Le Bihan, E. Breton, D. Lallemand, P. Grenier, E. Cabanis, and M. Laval-Jeantet, "MR imaging of intravoxel incoherent motions: Application to diffusion and perfusion in neurologic disorders," Radiology **161**, 401–407 (1986).

[15]A. J. E. Raaijmakers, B. W. Raaymakers, and J. J. W. Lagendijk, "Integrating a MRI scanner with a 6 MV radiotherapy accelerator: Dose increase at tissue-air interfaces in a lateral magnetic field due to returning electrons," Phys. Med. Biol. **50**, 1363–1376 (2005).

[16]D. C. Zheng, Y. B. Chen, Y. Chen, L. Y. Xu, F. J. Lin, J. Lin, C. B. Huang, and J. J. Pan, "Early assessment of induction chemotherapy response of nasopharyngeal carcinoma by pretreatment diffusion-weighted magnetic resonance imaging," J. Comput. Assisted Tomogr. **37**, 673–680 (2013).

[17]V. Vandecaveye, P. Dirix, F. De Keyzer, K. O. de Beeck, V. Vander Poorten, E. Hauben, M. Lambrecht, S. Nuyts, and R. Hermans, "Diffusion-weighted magnetic resonance imaging early after chemoradiotherapy to monitor treatment response in head-and-neck squamous cell carcinoma," Int. J. Radiat. Oncol., Biol., Phys. **82**, 1098–1107 (2012).

[18]B. W. Raaymakers *et al.*, "Integrating 1.5 T MRI scanner with a 6 MV accelerator: Proof of concept," Phys. Med. Biol. **54**, N229–N237 (2009).